Tetrahedron 68 (2012) 4517–4527

Contents lists available at SciVerse ScienceDirect

Tetrahedron

journal homepage: www.elsevier.com/locate/tet

Foldamers in pseudo[2]rotaxanes and [2]rotaxanes: tuning the switching kinetics and metastability

Kang-Da Zhang [a], Xin Zhao [a,*], Gui-Tao Wang [a], Yi Liu [b,*], Ying Zhang [c], Hao-Jie Lu [c,*], Xi-Kui Jiang [a], Zhan-Ting Li [a,c,*]

[a] State Key Laboratory of Bioorganic and Natural Products Chemistry, Shanghai Institute of Organic Chemistry, Chinese Academy of Sciences, 345 Lingling Lu, Shanghai 200032, China
[b] The Molecular Foundry, Lawrence Berkeley National Laboratory, One Cyclotron Road, Berkeley, CA 94720, USA
[c] Chemistry of Department, Fudan University, 220 Handan Road, Shanghai 200433, China

ARTICLE INFO

Article history:
Received 26 August 2011
Received in revised form 11 October 2011
Accepted 31 October 2011
Available online 6 November 2011

Keywords:
Foldamer
Hydrogen bond
Molecular device
Pseudorotaxane and rotaxane
Donor–acceptor interaction

ABSTRACT

Hydrogen bonded arylamide foldamers have been introduced in switchable pseudo[2]rotaxanes and [2]rotaxanes, which also include a cyclobisparaquat(*p*-phenylene) ($CBPQT^{4+}$) ring and a 'dumbbell' containing tetrathiafulvalene (TTF) and 1,5-dioxynaphthalene (DNP, for rotaxanes). The foldamer size changes through folding and unfolding serve as a steric handle to modulate the mechanical movement of the $CBPQT^{4+}$ ring along the dumbbell of the pseudo[2]rotaxanes and [2]rotaxanes. By varying the number of the repeating units in the foldamer, the kinetics of the solvent-dependent slippage/deslippage of pseudo[2]rotaxanes and the switching of the ring between TTF and DNP of the [2]rotoxanes can be tuned remarkably, with the time scope ranging from several minutes to several days, in twelve solvents of varying polarity, which have been confirmed by the ^{1}H NMR, UV–vis spectroscopy, and cyclic voltammogram experiments.

1. Introduction

[2]Rotaxanes are mechanically interlocked molecular architectures that consist of a linear 'dumbbell' component threaded through a macrocyclic 'ring' component.[1] The dumbbell component is typically equipped with bulky stoppers at both ends, with size larger than that of the ring component to prevent its extrusion.[2] Pseudo[2]rotaxanes are non-stoppered counterparts of rotaxanes—i.e., threaded complexes in which the linear dumbbells bear end groups that have smaller sizes than the ring components.[3] One of the most important features of pseudo-[2]rotaxanes and [2]rotaxanes is that their ring component can extrude or shuttle along the linear dumbbell.[4] When the dumbbell component is incorporated with two or more 'stations' with different recognition strength, selective positioning of the ring component over the stations can be realized to give molecular systems with multiple states.[5] In the past two decades, bi- and multi-stable supramolecular systems of this kind have received great attention due to their applications in the construction of molecular machines and devices.[2b,6] Particularly, the potential application in high density molecular memories concerns bistable [2]rotaxanes incorporating redox-active tetrathiafulvalene (TTF), 1,5-dioxynaphthalene (DNP), and cyclobis(paraquat-*p*-phenylene) ($CBPQT^{4+}$),[7] which have been sandwiched inside molecular switch tunnel junction (MSTJ) devices in extended cross-bar networks.[7b] One issue associated with these MSTJ devices is their short lifetime due to the relaxation of the molecules from its metastable state co-conformation (MSCC) to the ground state co-conformation (GSCC). In order for these MSTJ devices to store information as non-volatile memory, one has to generate a long-lived MSCC of the [2]rotaxanes even after removal of the bias. This could be done by introducing a barrier between the TTF and DNP units to slow down the back shuttling of the $CBPQT^{4+}$ ring from the DNP unit to the neutral TTF unit. The barrier should be prudently adjusted, however, to an appropriate level such that the forward shuttling of the $CBPQT^{4+}$ ring from the oxidized TTF unit to the DNP unit is not slowed down significantly. The medium itself can affect the barrier for the original [2]rotaxanes, with the barrier energy being from 16 kcal/mol in solution to 18 kcal/mol in polymer gel and 21 kcal/mol in the solid state device.[8] More recently, charged spacer units have been utilized to raise the barrier for the movement of the $CBPQT^{4+}$ ring by producing an electrostatic repulsion, and an activation barrier in solution of 19 kcal/mol is reached when a bipyridinium spacer is used.[7b,9] Another desirable approach is the use of deformable foldamer spacers as steric barriers to endow extra stability for the MSCC.

* Corresponding authors. Tel.: +86 21 54925122; fax: +86 21 64166128; e-mail addresses: xzhao@mail.sioc.ac.cn (X. Zhao), ztli@mail.sioc.ac.cn (Z.-T. Li).

0040-4020/$ – see front matter © 2011 Elsevier Ltd. All rights reserved.
doi:10.1016/j.tet.2011.10.116

Foldamers are linear molecules or oligomers that adopt a secondary structure, typically a folded or helical one, stabilized by discrete noncovalent interactions.[10–12] The folding and unfolding process is reversible, involving either energy release or consumption. The folded states, like the helix of natural peptides, have an apparent size larger than that of the extended ones. On the base of this feature, we have recently utilized hydrogen bonded arylamide foldamers to tune the dynamic mechanical property of methacrylate copolymers.[13] We conjectured that, if the apparent diameter of the extended state of a foldamer is smaller than the internal diameter of a macrocycle while the diameter of its folded state is larger, it would be possible for the macrocycle to slip over the linear foldamer when extended. However, the slippage should be decelerated compared to that over a similar but flexible molecule, because it needs to, at least partially, break the noncovalent bonds existing in the folded state. Since the length of foldamers can be readily modulated by simply changing the number of their repeating units, the folded segments could be utilized as new modular stoppers or spaces for regulating the dynamic behavior of pseudorotaxanes or rotaxanes.

Herein, we describe a systematic investigation of the kinetic properties of two series of foldamer-containing interlocked species, which are stabilized by the intermolecular donor–acceptor interaction between the TTF unit and the $CBPQT^{4+}$ ring.[14,15] The first series are pseudo[2]orotaxanes where a hydrogen bonding-driven arylamide foldamer segment is attached as stopper at one of the two ends of the dumbbell component. Three of these threaded complexes can be isolated as stable pseudo[2]rotaxanes in the solid state, and are shown to display half-lives ranging from 2.7 s to more than 22 days, depending on the length of the foldamer segment and the polarity of the medium.[16] Based on these model pseudo[2] rotaxane systems, we have extended our studies toward bistable [2] rotaxanes, in which a foldamer segment is incorporated to connect a TTF unit and a DNP unit in the dumbbell component.[17] The foldamer segments as deformable spacers are shown to effectively tune the shuttling of the $CBPQT^{4+}$ ring between the TTF, in both its neutral and oxidized forms, and DNP units.[18] Consequently, the lifetime of the post-oxidation MSCC in solution is dramatically increased.[19]

2. Results and discussion

2.1. Design and synthesis

Chart 1 lists the structures of foldamer-containing pseudo-[2] rotaxanes **1a**–**d** and bistable [2]rotaxanes **2a** and **2b**, and the corresponding dumbbell components **3a**–**d**, **4a**, and **4b**. We chose to utilize the well-known TTF-$CBPQT^{4+}$ donor–acceptor recognition motif for the present study because (i) the donor–acceptor interaction lives in both polar and less polar solvents, (ii) TTF unit has reversible redox behavior, and (iii) the kinetics related to this motif can be investigated using UV–vis, ^{1}H NMR, and cyclic voltammogram techniques. Because the foldamer conformation is highly solvent dependant, the solubility control was crucially important for the investigation of the effect of the foldamer segments on the dynamic properties of the threaded complexes. The large Fréchet-

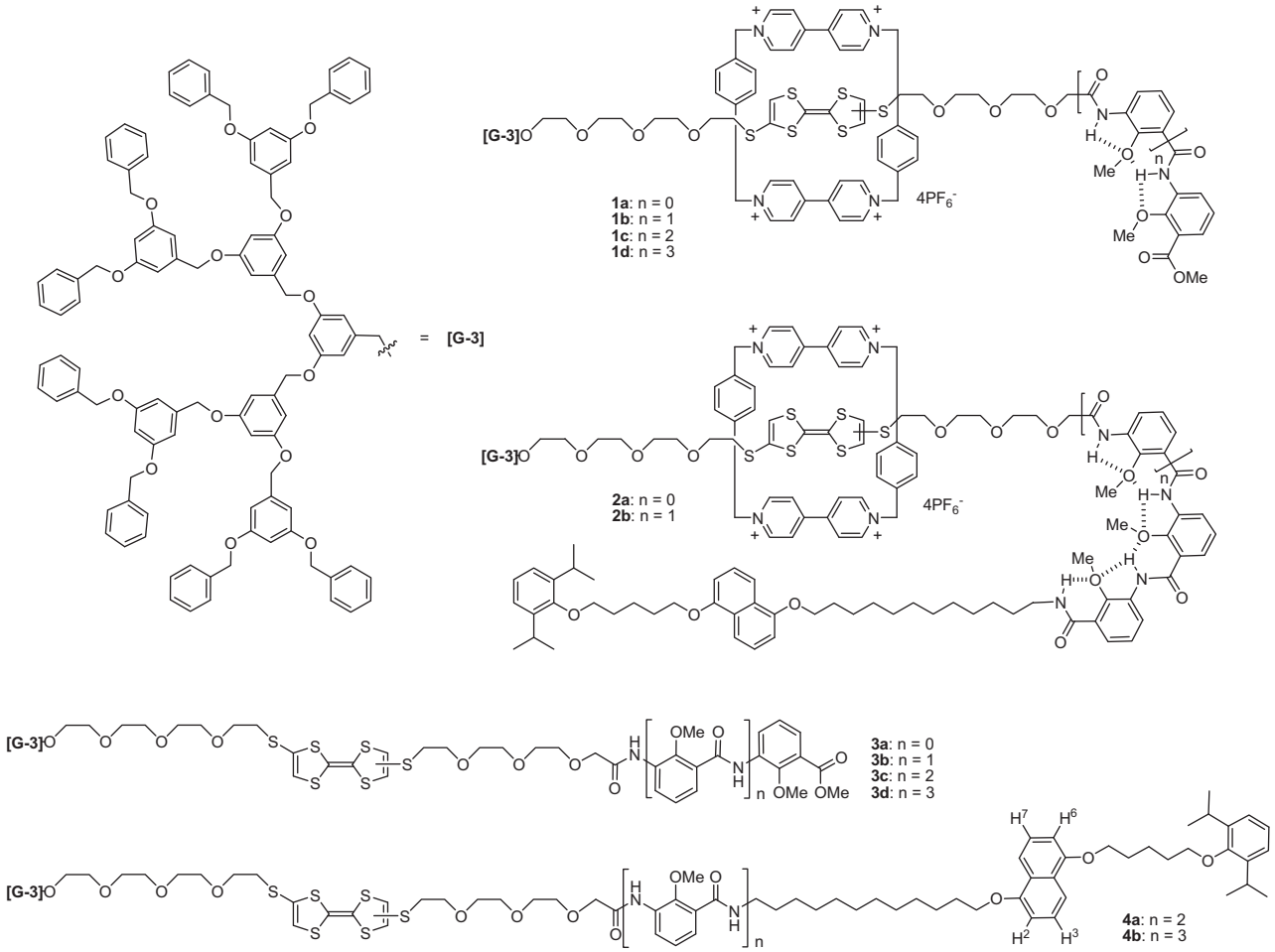

Chart 1. The structures of foldamer-containing pseudo[2]rotaxanes **1a**–**d**, bistable [2]rotaxanes **2a** and **2b**, and thread molecules **3a**–**d**, **4a** and **4b**.

type **G-3** dendron was thus introduced to one of the two ends of the linear components to ensure good solubility for the tetracationic interlocked molecules in both less polar and polar solvents.[20,21] Foldamer segments of varying length are introduced to another end of the linear components. There are a number of hydrogen bonded folding patterns available as stopper groups. We chose the 3-amino-2-methoxybenzoic acid-derived foldamers[22] because this folding pattern survives a range of solvents,[22b] and in these foldamers, five repeating units form one turn,[23] endowing short oligomers with a large apparent size through folding. A systematic investigation of the length-dependence of the dynamic property would reveal their function as tunable steric barrier for controlling the extrusion or slippage of the $CBPQT^{4+}$ ring (Fig. 1). Molecular modeling reveals that a single 2-methoxyl 1,3-benzamide repeating unit in the foldamer segment is not bulky enough to prevent the extrusion of the $CBPQT^{4+}$ ring, while the folded structure as a whole is. The two oligo(ethylene glycol) chains linking the TTF unit and the end groups are expected to strengthen the TTF-$CBPQT^{4+}$ complexation through the formation of intermolecular C–H···O hydrogen bonds between the pyridinium protons and the neighboring ether oxygen atoms.[24] For [2]rotaxanes **2a** and **2b**, the electron-rich DNP unit is incorporated in the dumbbell to form a foldamer-bridged bistable system (Fig. 6, vide infra). The 1,3-diisopropyl-phenoxyl group is used as the other stopper to prevent the extrusion of the $CBPQT^{4+}$ ring.[25]

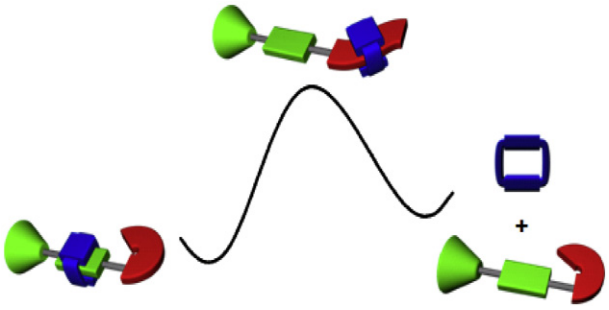

Fig. 1. Schematic representation depicting the foldamer-modulated extrusion (pseudo [2]rotaxane decomplexation) or slippage (pseudo[2]-rotaxane formation) of the $CBPQT^{4+}$ ring from or onto a TTF-containing thread. The foldamer segment (red) in its folded state has a large apparent size and must unfold into an extended conformation in order for the $CBPQT^{4+}$ ring to pass over.

Linear compounds **3a**–**d** were prepared according to the routes shown in Scheme 1. Tetraglycol **5** was first reacted with [**G-3**]Br **6**[20] in tetrahydrofuran (THF) in the presence of sodium hydride to give **7** in 94% yield. The alcohol was then treated with tosyl chloride in dichloromethane in the presence of potassium hydroxide to produce **8** in 92% yield, which was transformed quantitatively into the corresponding iodide **9** after treatment with sodium iodide in acetone. Its reaction with **10**[26] in THF and methanol was activated by cesium hydroxide to give **11** in 73% yield. Iodide **13**, obtained from treating tosylate **12** with sodium iodide in acetone, was subjected to the reaction of **11** in the presence of cesium hydroxide to produce **14** in 80% yield. After hydrolysis in aqueous THF, the carboxylic acid **15** was first converted to carbamate, followed by coupling with **16a**–**d**,[23a] to produce **3a**–**d** in 52–70% yields.

The preparation of pure threaded complexes **1a**–**d** from **3a**–**d** and $CBPQT{\cdot}4PF_6$[24] was then exploited. It was postulated that, once the complexes were formed by the slippage of the $CBPQT^{4+}$ ring over the foldamer segment, the large **G-3** dendron would ensure good solubility for these complexes in less polar solvents. Provided the reverse extrusion process was slow enough, one could separate the pure complexes from the two free species by simply making use of their difference in solubility. This was proven the case for threaded complexes **1b**–**d**. The 1:1 mixtures of threads **1b**–**d** with $CBPQT{\cdot}4PF_6$ in a minimal amount of acetonitrile and acetone (1:2, v/v) were stirred for 48 h and then concentrated at ambient temperature. The resulting green residue was then triturated with a minimal amount of more polar acetonitrile and water (1:4, v/v) to remove free $CBPQT{\cdot}4PF_6$. The

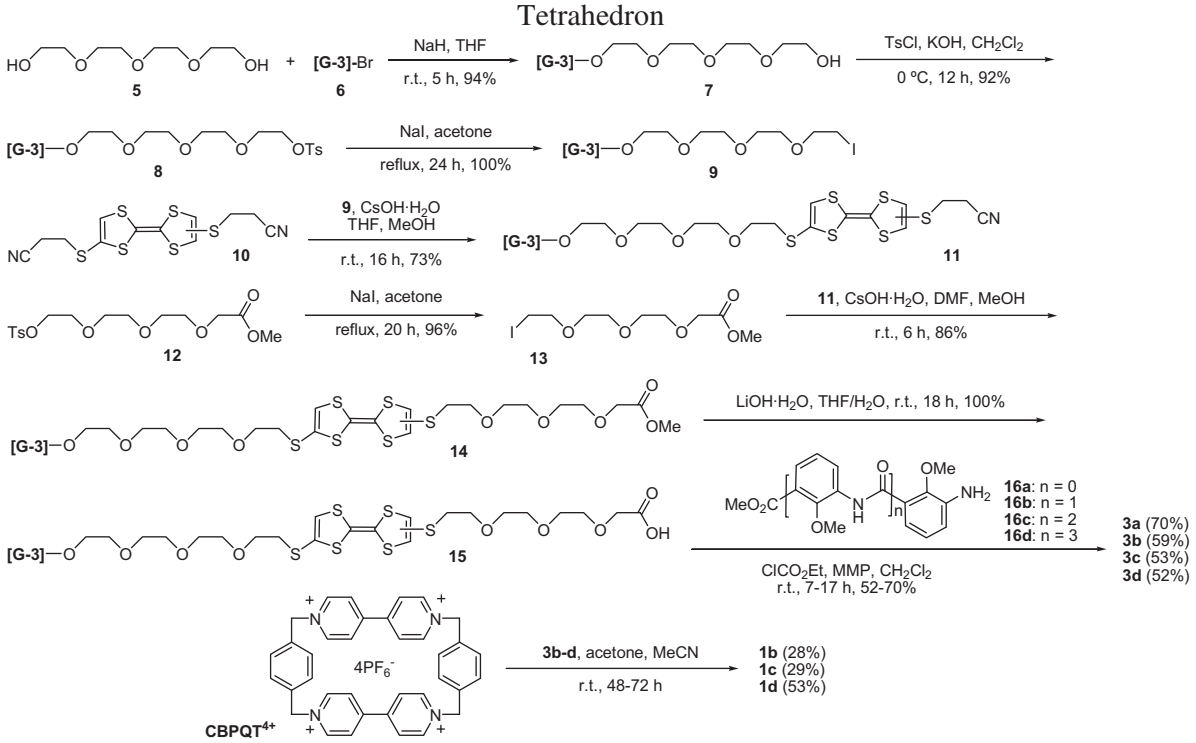

Scheme 1. The synthesis of threads **3a**–**d** and pseudo[2]rotaxanes **1b**–**d**.

remaining green solid was further triturated with a mixture of less polar dichloromethane and petroleum ether (1:2, v/v) to remove un-reacted threads **1b**–**d**. Threaded complexes **1b**–**d** could thus be obtained as green solids in 28%, 29%, and 53% yields, respectively, as confirmed by ^{1}H NMR spectroscopy (vide infra). All the three pseudorotaxanes remain as stable complexes in the solid state.[27] Pseudo[2]rotaxane **1a** could not be isolated in its pure interlocked form using the similar procedure as a result of fast decomplexation.[28]

The synthetic routes for [2]rotaxanes **2a** and **2b** and dumbbells **4a** and **4b** are described in Scheme 2. Phenol **17** was first reacted with 1,5-dibromopentane in acetonitrile to give compound **18** in 87% yield. The bromide was then treated with 1,5-dihydroxynaphthalene in ethanol with potassium hydroxide as base to afford **19** in 56% yield. This naphthol was further coupled with bromide **20** in acetonitrile in the presence of potassium carbonate to produce **21** in 79% yield. Treatment of compound **21** with hydrazine in ethanol quantitatively yielded **22**, which was further coupled with acid **23a** and **23b**[23] to produce **24a** and **24b** in 78% and 43% yields, respectively. Pd-catalyzed hydrogenation of the two nitro compounds in THF and chloroform generated **25a** and **25b** in nearly quantitative yields. The two amines were then coupled with **15**, which was activated with ethyl chloroformate, in the presence of CBPQT·4PF$_6$ to produce both [2]rotaxanes **2a** and **2b** and dumbbell **4a** and **4b** in moderate yields.

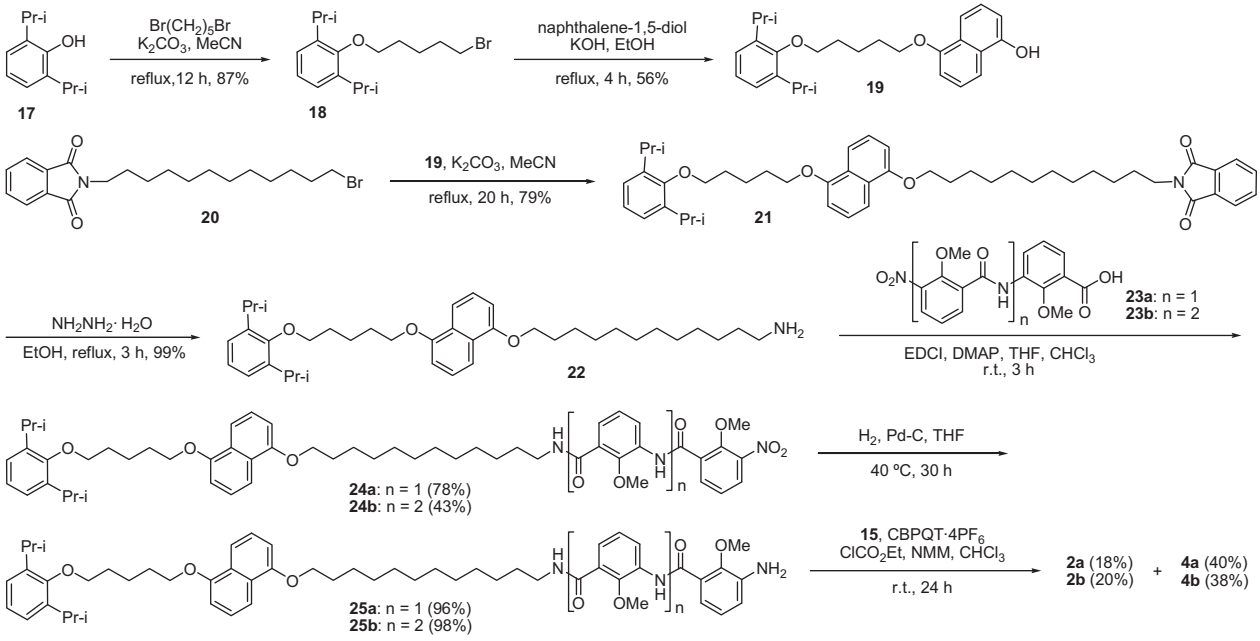

Scheme 2. The synthesis of [2]rotaxanes **2a** and **2b** and threads **4a**–**d**.

2.2. Association constants of threaded complexes 1a–d

The ^{1}H NMR spectra of complexes **1c** and **1d** in acetonitrile-d_3 displayed one set of signals, which was attributed to the pseudorotaxanes because (i) resonances corresponding to both CBPQT^{4+} and dumbbell components were observed, but none of them were from the individual free species, suggesting that they were complexed, (ii) the two components existed in a 1:1 ratio, as indicated by the relative intensity of their respective resonances. After standing for a period of time, the resonances of the free components appeared gradually, while those of the complexes diminished. Equilibria for **1c** and **1d** were reached after different standing times. On the other hand, the ^{1}H NMR spectrum of complex **1b** in acetonitrile-d_3 recorded immediately after it was dissolved already exhibited the signals of both free and complexed **3b** and CBPQT·4PF$_6$, reflecting that it underwent a more rapid decomplexation process.

The slippage of the CBPQT^{4+} ring over the foldamer segments of **3a**–**d** to form the threaded complexes were also followed by recording the ^{1}H NMR spectra of their 1:1 solution in acetone-d_6, acetonitrile-d_3, and DMSO-d_6 at different time intervals. As expected, the process was revealed to be time-dependent. The time for reaching equilibrium increased with the elongation of the foldamer segment and was shorter in DMSO-d_6 than in acetonitrile-d_3 or acetone-d_6. In all cases, the resonances of the pyridinium β-H of the free and threaded CBPQT^{4+} ring did not overlap with others, which were assigned by comparing the spectra with those of pure CBPQT·4PF$_6$ and previously reported related threaded systems.[29] On the base of the relative intensities of these signals, we determined the association constants (K_a) of the threaded complexes, which, together with the calculated free energies of complexation (ΔG°), are provided in Table 1. The same results were obtained starting from preformed complexes **1b**–**d** after the samples were allowed to stand for enough time. The values are comparable to those reported for other pseudo-[2]rotaxanes stabilized by the TTF-CBPQT^{4+} donor–acceptor interactions,[14] suggesting that the

Table 1
The association constants (K_a) of pseudo[2]rotaxanes **1a**–**d** and the associated free energies (ΔG°) at 25 °C

	1a		**1b**		**1c**		**1d**	
	K_a (M^{-1})	ΔG° (kJ/mol)	K_a (M^{-1})	ΔG° (kJ/mol)	K_a (M^{-1})	ΔG° (kJ/mol)	K_a (M^{-1})	ΔG° (kJ/mol)
Acetonitrile-d_3	1800	−18.6	752	−16.4	868	−16.8	576	−15.7
Acetone-d_6	420	−15.0	258	−13.8	411	−14.9	187	−13.0
DMSO-d_6	146	−12.3	157	−12.5	152	−12.4	120	−11.9

foldamer segments did not play a significant role in determining the thermodynamic stability of these pseudo[2]rotaxanes.

2.3. Extrusion kinetics of CBPQT^{4+} of pseudo[2]rotaxanes 1a–d

The above ^{1}H NMR investigations revealed that foldamer-capped pseudo[2]rotaxanes can exhibit [2]rotaxane-like characters, depending on the foldamer segments in the threads and the media. To get deep insight into the effect of the foldamer segments and the media on the dynamic properties of the threaded complexes, a systematic kinetic investigation was performed. The TTF-CBPQT^{4+} charge-transfer (CT) absorption, centered on 805 nm in the UV–vis spectra, was used as the probe.[16] By monitoring the decrease of this CT absorption with time, we obtained the rate constants (k_{off}) of the decomplexation of the pseudo[2]rotaxanes in twelve solvents, from highly polar DMSO and DMF to less polar chloroform, by assuming a first-order kinetics. The data, together with the associated change of free energy and half-life values, are listed in Table 2. The rates of decomplexation of pseudo[2]rotaxane **1a** could not be determined using this method because the process was too rapid to be monitored by the UV–vis spectroscopy. Thus, we first used the UV–vis experiments to measure the rates of formation (k_{on}) of the pseudorotaxane from **3a** and CBPQT·4PF$_6$ in polar DMSO, acetonitrile and acetone, and then calculated the k_{off} values in these solvents (0.058, 0.19, and 0.26 s^{-1}, respectively) using the equation $k_{off}=k_{on}/K$, where K was the association constant of the complex (Table 1).[30] The value in less polar solvents could not be obtained due to the low solubility of CBPQT·4PF$_6$.

Compared with those of **1a** in the same solvent, the k_{off} values of **1b** decreased considerably, by as large as 58 to 365 times. The extent of rate drop became smaller from **1b** to **1c**, being 5 to 37 times, and even smaller from **1c** to **1d**, being only two to five times. These observations indicated that all the hydrogen bonded arylamide units in the foldamer segments contributed in delaying the extrusion of CBPQT^{4+}, but not in a cooperative manner. Since the depth of the CBPQT^{4+} ring is shorter than the width of the arylamide repeat, for the longer foldamer segments in **1c** and **1d**, we proposed that the extrusion of the CBPQT^{4+} ring does not require simultaneous breaking of all the hydrogen bonds. Instead, it should be a multi-step process, which involved successive breaking of the hydrogen bonds, probably mainly the six-membered ones, of one arylamide unit after another from the TTF side. As illustrated in Fig. 2, the extrusion of the CBPQT^{4+} ring only break the hydrogen bonds of the arylamide unit close to the edges of its cavity, commensurate with the conformational change of the encircled segment. The whole process is, to some extent, like removing a ring from a curved, sticky finger over knuckles. The five-membered N–H···O hydrogen bonds might survive, at least partially, during the extrusion because the breaking of this series of hydrogen bonds does not cause a size decrease, but would lead to the formation of the cis conformation of the N–C(Ar) bond, which is unfavorable as a result of the electrostatic repulsion between the neighboring C=O and methoxyl oxygen atoms.

It has been established that the donor–acceptor interactions between the TTF and bipyridinium units become weakened pronouncedly in less polar solvents due to the decrease of their π-stacking interation.[31] The decomplexation of pseudo[2]rotaxanes

Table 2
The kinetic data for the extrusion of the CBPQT^{4+} ring over the foldamer segments in pseudo[2]rotaxanes **1b**–**d** at 25 °C in different solvents

Solvent	ε[a]	β[b]	**1b**			**1c**			**1d**		
			k_{off} (s^{-1})	$\Delta G^{\neq}$ (kJ/mol)	Half-life (s)	k_{off} (s^{-1})	$\Delta G^{\neq}$ (kJ/mol)	Half-life (s)	k_{off} (s^{-1})	$\Delta G^{\neq}$ (kJ/mol)	Half-life (s)
DMSO	47.2	0.76	1.0×10^{-3}	90	6.9×10^{2}	1.1×10^{-4}	96	6.3×10^{3}	4.0×10^{-5}	98	1.7×10^{4}
DMF	36.7	0.69	2.3×10^{-3}	88	3.0×10^{2}	4.7×10^{-4}	92	1.7×10^{3}	1.0×10^{-4}	96	6.9×10^{3}
MeCN	38.3	0.41	5.2×10^{-4}	92	5.3×10^{4}	4.0×10^{-5}	98	1.7×10^{4}	9.7×10^{-6}	102	7.1×10^{4}
PhCN	25.7	0.41	2.8×10^{-4}	93	2.5×10^{3}	2.0×10^{-5}	100	3.5×10^{4}	8.9×10^{-6}	102	7.8×10^{4}
Acetone	21.0	0.48	8.4×10^{-4}	91	8.2×10^{2}	1.3×10^{-4}	95	5.3×10^{3}	2.5×10^{-5}	99	2.8×10^{4}
Butanone	18.6	0.48	6.6×10^{-4}	91	1.0×10^{3}	6.0×10^{-5}	97	1.2×10^{4}	3.0×10^{-5}	99	2.3×10^{4}
Cyclohexanone	16.1	0.53	7.8×10^{-4}	91	8.8×10^{2}	6.0×10^{-5}	97	1.2×10^{4}	2.0×10^{-5}	100	3.5×10^{4}
Cyclopentanone	13.6	0.52	7.5×10^{-4}	91	9.2×10^{2}	6.0×10^{-5}	97	1.2×10^{4}	3.0×10^{-5}	99	2.3×10^{4}
$ClCH_2CO_2Et$	11.4	0.35	1.0×10^{-4}	96	6.9×10^{3}	6.7×10^{-6}	103	1.0×10^{5}	2.6×10^{-6}	105	2.7×10^{5}
$ClCH_2CH_2Cl$	10.4	0	7.5×10^{-6}	102	9.2×10^{4}	2.0×10^{-7}	111	3.5×10^{6}	5.1×10^{-7}[c]	115	1.4×10^{6}[c]
THF	7.5	0.55	2.6×10^{-4}	94	2.7×10^{3}	8.3×10^{-6}	102	8.5×10^{4}	2.1×10^{-6}	105	3.3×10^{5}
Chloroform	4.8	0.10	1.9×10^{-6}	106	3.6×10^{5}	1.2×10^{-7}	113	5.8×10^{6}	3.6×10^{-7}[c]	116	1.9×10^{6}[c]

[a] Dielectric constant of the solvent.
[b] Scale of the solvent as a hydrogen bond acceptor.
[c] Measured at 40 °C.

As expected, the decomplexation of the pseudo[2]rotaxanes in the same solvent decelerated with the elongation of the foldamer segments and, for the same pseudo[2]rotaxane, accelerated with the increase of the solvent polarity. For example, **1a** decomposed very quickly, with a half-life of as short as 2.7 s in acetone. In contrast, **1d** was much more stable in chloroform and 1,2-dichloroethane. Indeed, it was found that even after standing for 4 days at ambient temperature, its CT absorption still exhibited no perceptible decrease, indicating that it had a rotaxane-like character in these two solvents. It started to slowly decomplex at 40 °C, with the half-lives still being as long as 22 and 16 days (Table 2) in the two solvents. Thus, by choosing foldamer segments of varying length and solvents of different polarity, we could control the extrusion of the CBPQT^{4+} ring from the threads in a remarkably long span of time.

1b–**d** was substantially slower in less polar solvents (such as chloroform) than in polar solvents (such as DMSO and DMF), suggesting that the increase of the free energy from a polar solvent to a less polar solvent was obviously smaller than the increase of the free energy of activation for the extrusion of the CBPQT^{4+} ring from the linear component caused by the enhancement of the intramolecular hydrogen bonds of their foldamer segment in less polar solvent. The fact that all the threaded complexes decomplexed even in less polar solvents suggests that they are all pseudo[2]rotaxanes, but have an increased character of [2]rotaxanes with the introduction of longer foldamer segment in the threads. No linear relationship is observed between the k_{off} values and the dielectric constant (ε) or the β scale—the ability of a solvent as a hydrogen bonding acceptor (Table 2).[32] This observation is, however, not unexpected considering that the TTF-CBPQT^{4+} donor–acceptor

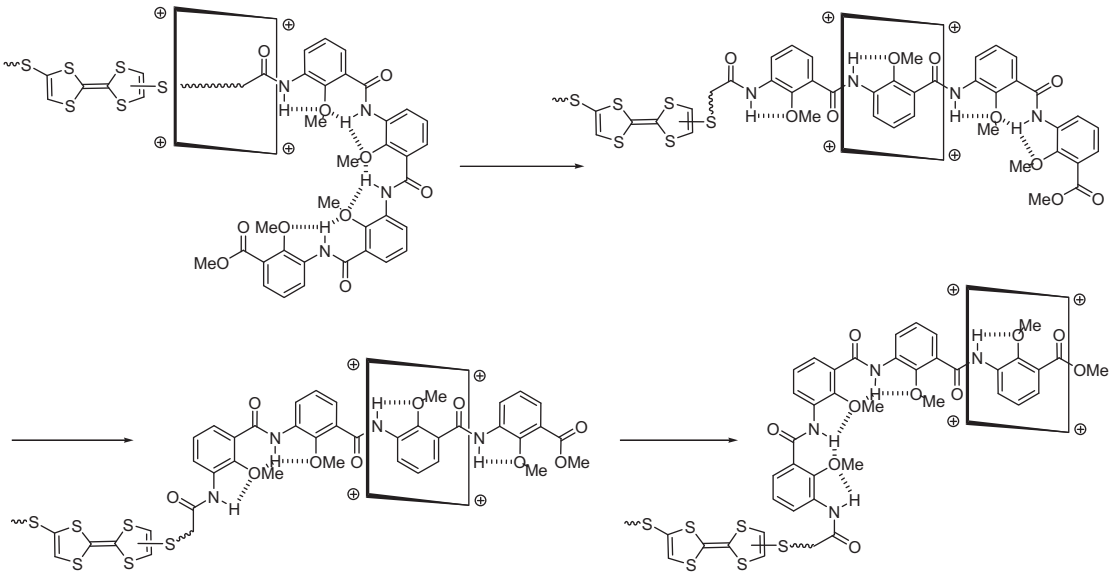

Fig. 2. Proposed multi-step extrusion mechanism of the $CBPQT^{4+}$ ring from the thread in **1d**, which involves the breaking and re-formation of the six-membered intramolecular N–H···O hydrogen bonds in the foldamer segments.

interactions and the intramolecular N–H···O hydrogen bonding of the foldamer segment are dependent on multiple factors. It is noteworthy that the ε value of THF is between those of chloroform and 1,2-dichloroethane, but its β scale is much higher than those of the two chlorinated solvents, which should account for the observation that the rates of decomplexation for all the pseudo[2]rotaxanes in THF are substantially larger than those in the chlorinated solvents.

2.4. Kinetic isotope effect of the extrusion of $CBPQT^{4+}$ of 1b

Since the extrusion of the $CBPQT^{4+}$ ring from the threads of the pseudo[2]rotaxanes was highly dependent on the hydrogen bonded foldamer segment of their thread component, this process might exhibit a kinetic isotope effect (KIE) if the amide hydrogens were exchanged to deuteriums. The zero-point free energy of the resulting N–D···O deuterium bonding is expected to decrease with respect to that of the N–H···O hydrogen bonding of the same amide in the threaded state. During the extrusion process (Fig. 2), both the hydrogen and deuterium bondings would be weakened or broken. As a result, the difference between their zero-point free energies should decrease, or even close to zero if they were broken completely, as shown in Fig. 3. To testify this, deuterium exchange was conducted for **3b** by sonicating its solution in the mixture of $CDCl_3$, DMSO-d_6, and D_2O (47.5:47.5:5 v/v/v), which was monitored by ^1H NMR. After the disappearance of the amide signals, the pure sample was separated and used to prepare pseudo[2]rotaxane **1b** with deuterated amide units. The k_{off} values of this deuterated **1b** in four polar solvents were measured using UV–vis spectroscopy and the results listed in Table 3. It can be seen that the kinetic isotope effect (KIE) increases notedly with the decrease of the solvent polarity, supporting that the intramolecular N–H···O hydrogen bonding is present in these solvents and plays its role in modulating the extrusion of the $CBPQT^{4+}$ ring.[22b,33]

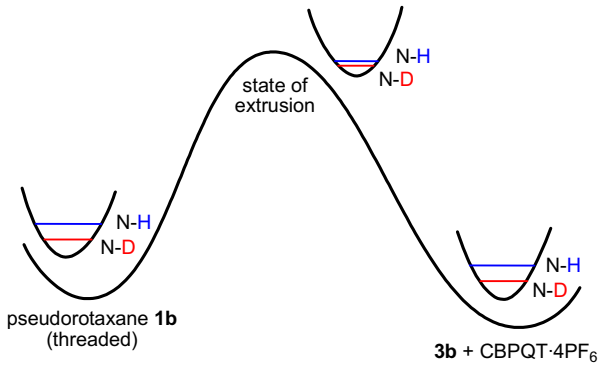

Fig. 3. The mechanism for the kinetic isotope effect of the decomplexation of foldamer-derived pseudorotaxane **1b**.

Table 3
The kinetic data for the decomplexation of deuterated **1b** at 25 °C in different polar solvents and the related kinetic isotope effect

	DMF	MeCN	Acetone	THF
k_D	2.1×10^{-3}	6.1×10^{-4}	3.7×10^{-4}	1.7×10^{-4}
KIE[a]	1.1	1.4	1.4	1.5

[a] KIE represents the k_H/k_D ratio.

2.5. TTF redox chemistry and extrusion kinetics of the $CBPQT^{4+}$ ring off pseudorotaxanes 1b–d

Cyclic voltammetry (CV) was used to investigate the redox property of the TTF unit in pseudo[2]rotaxanes **1b–d** in both less polar chloroform and polar acetonitrile. The first oxidation potential of the three samples in chloroform was all 0.65 V, which was larger than that (0.53 V) of control compound **3b**,[17] reflecting the decreased electron-donating ability of the complexed TTF unit with respect to the free one. The second oxidation potential of both **1b–d** and **3b** in chloroform was all 0.84 V, implying that the formation of radical cation $TTF^{+\bullet}$ had forced the $CBPQT^{4+}$ ring of **1b–d** to slip off the TTF unit and hence the $CBPQT^{4+}$ ring did not affect the TTF^{2+} dicationic ion formation. The electrochemical behavior is quite different in acetonitrile. Pseudo[2]rotaxanes **1b–d** exhibited only one oxidation process at 0.77 V, whereas **3b** still gave rise to two peaks at 0.44 and 0.78 V, respectively (Fig. 4). The CV of **1b** recorded in acetonitrile showed an additional weak broad peak at 0.44 V, assignable to the oxidation of free TTF unit. Such peak was

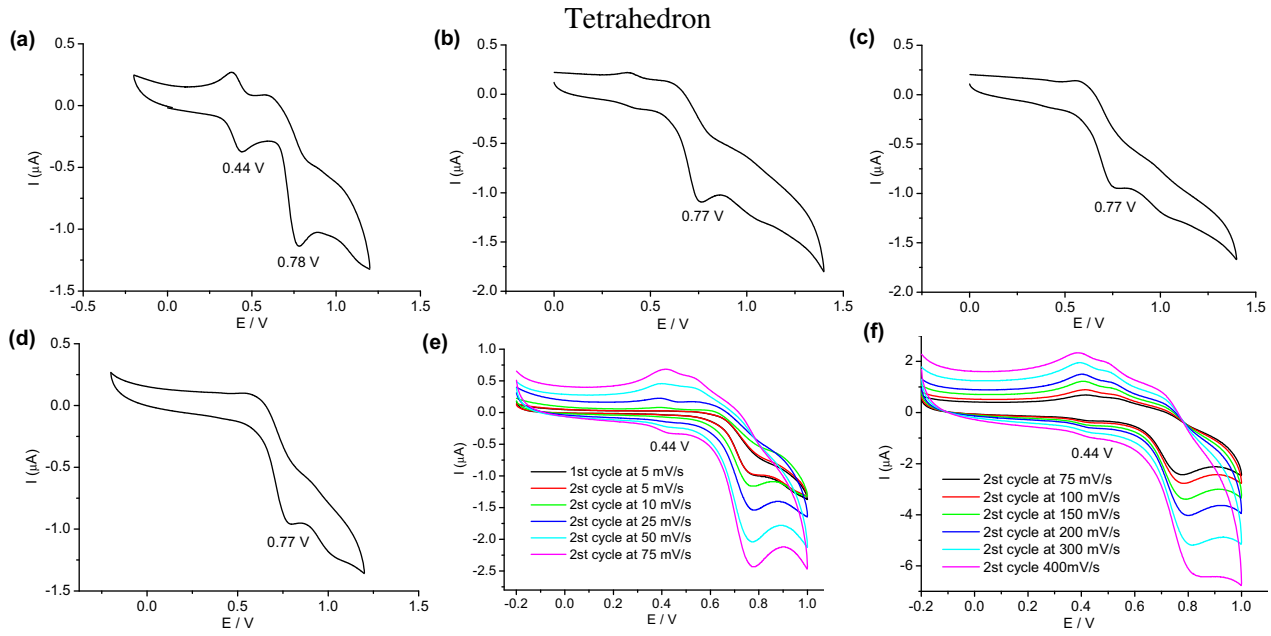

Fig. 4. CVs (0.1 mM, scan rate=10 mV/s) of (a) **3b**, (b–d) pseudo[2]rotaxanes **1b**–**d** in MeCN at 25 °C, (e,f) CVs of bistable [2]rotaxane **2a** (0.1 mM) at different scan rates in MeCN at 25 °C. The Pt button and coil and Ag/AgCl electrodes were used as working, counter, and reference electrodes. *n*-$Bu_4N{\cdot}PF_6$ (0.1 M) was used as the electrolyte.

not observed for **1c** and **1d** in acetonitrile and for all the three pseudo[2]rotaxanes in chloroform. These results indicated that, within the time scale of the electrochemical measurement, **1b** already started to decomplex in acetonitrile but remained intact in chloroform during the redox cycle, while **1c** and **1d** were more stable in either solution conditions, which were consistent with the above UV–vis kinetic experiments.

The redox-activated dynamic process was also investigated using the chemical oxidation/reduction methods. Adding 2.0 equiv of Magic Blue ($(4\text{-}BrC_6H_4)_4N^+SbCl_6^-$)[16,34] or 1.0 equiv of $Fe(ClO_4)_3$ to the solution of pseudo[2]rotaxanes **1b**–**d** in acetonitrile resulted in the oxidation of the TTF unit to TTF^{2+} or $TTF^{+\bullet}$.[29] The kinetics of decomplexation of these oxidized pseudo[2]rotaxanes was then investigated using the UV–vis spectroscopy. By assuming a first-order kinetic process for the extrusion of the $CBPQT^{4+}$ ring over the foldamer segment, we derived the k_{off} values using the equation $k_{off}=[\ln(C_0/C)]/t$, where C_0 and C were the initial concentration and the concentration of the threaded complexes at time t, which approximately equaled the time interval between the oxidation and reduction of the sample. To reach the reduced state, the solutions of the oxidized pseudo[2]rotaxanes were treated with an excess of zinc powder. The recovered CT absorptions of the remaining pseudo-[2]rotaxanes were recorded, and the C values were obtained by comparing the absorptions with those of the initial solutions. Alternatively, the C_0/C could be obtained using the ^1H NMR spectroscopy by comparing the relative integrated intensity of the CH_2 signals of the free and complexed $CBPQT^{4+}$ ring (Fig. 5a–c). The k_{off} values of decomplexation were listed in Table 4. It can be seen that, for the same pseudo[2]rotaxane, the k_{off} values for the oxidized complex are comparable and independent on the oxidation state of TTF unit. Since the electrostatic repulsion between TTF^{2+} and $CBPQT^{4+}$ should be larger than that between $TTF^{+\bullet}$ and $CBPQT^{4+}$, this observation supports that the energy barrier for extrusion of the $CBPQT^{4+}$ ring, after the first oxidation of TTF, was predominantly controlled by its deslippage over the bulky foldamer segment. This result may be attributed to the long linker between the TTF and foldamer unit, which allowed the $CBPQT^{4+}$ ring to rapidly escape far away from the oxidized TTF unit. The corresponding charge repulsion decayed exponentially to an insignificant level when compared to the energy cost for the $CBPQT^{4+}$

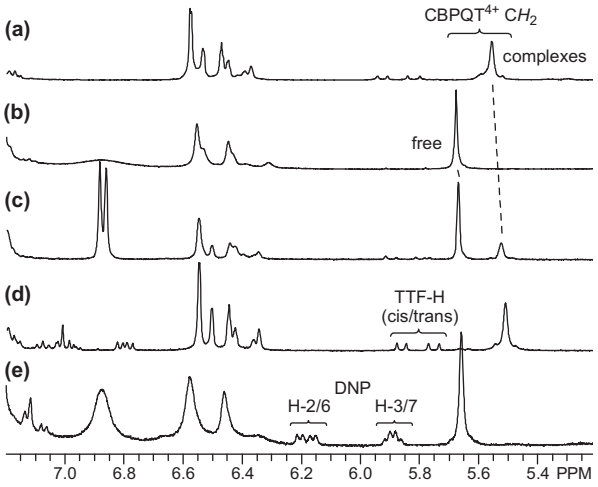

Fig. 5. Partial ^1H NMR spectra (400 MHz, aceotonitrile-d_3, 25 °C) of (a) pseudo[2]rotaxane **1d**, (b) **1d** after Magic Blue (2.0 equiv) was added, (c) **1d** recorded after zinc powder (5.0 equiv) was added to the above solution of **1d** and Magic Blue, which was first allowed to stand for 5 min (without this reduction process, ^1H NMR showed no difference for the signals of the free and complexed $CBPQT^{4+}$ ring), and (d) bistable [2]rotaxane **2a** and (e) **2a** after Magic Blue (2.0 equiv) was added for 5 min. The concentration for **1d** and **2a** were kept at 2.0 mM.

Table 4
The kinetic data for the decomplexation of mono- ($TTF^{+\bullet}$) and dioxidized (TTF^{2+}) pseudorotaxanes **1b**–**d** in acetonitrile at 25 °C, measured by the UV–vis method

	$k_{off}(TTF^{+\bullet})$ (s^{-1})	Half-life (s)	$k_{off}(TTF^{2+})$ (s^{-1})	Half-life (s)
1b	0.11	6.3	0.11	6.3
1c	0.016	43	0.020	37
1d	0.0042	165	0.0042	165
1d			0.0045[a]	154
1d			0.0081[b]	66

[a] Determined in acetonitrile-d_3 using the ^1H NMR method.
[b] Value determined in acetone.

ring slipping over the foldamer segment. On the other hand, the k_{off} values of the mono- and dioxidized **1b**–**d** in acetonitrile were 212–433 times higher than the values of the corresponding unoxidized samples in the same solvent (Table 2). The kinetic stability in the unoxidized pseudo[2]rotaxanes was attributed to the TTF-CBPQT^{4+} donor–acceptor interaction.

2.6. Bistable [2]rotaxanes 2a and 2b

Since the dimeric and trimeric foldamer segments in pseudo[2]rotaxanes **1b** and **1c** could provide an energy barrier for the CBPQT^{4+} ring to extrude at a rate of 10^{-2}–10^{-7} s^{-1}, we further prepared bistable [2]rotaxanes **2a** and **2b** to study the foldamer-tuned switching of the CBPQT^{4+} ring between the TTF and DNP sites (Fig. 6). For most of previously reported TTF/DNP–CBPQT^{4+} bistable [2]rotaxanes,[17] the TTF and DNP sites are connected with short chains, hence the shuttling of CBPQT^{4+} between the two sites is usually rapid. Since TTF is more electron-rich than DNP, in a two-state model, the equilibrium is always shifted toward the CBPQT^{4+} ring encircling the TTF site to form GSCC, rather than toward the

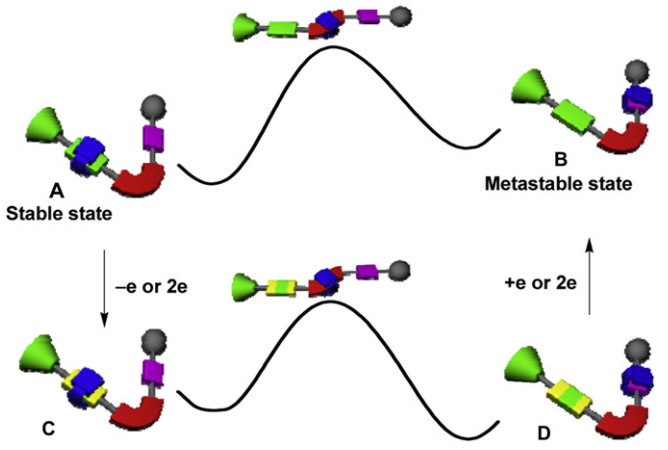

Fig. 6. Schematic representation depicting the foldamer-tuned switching of the CBPQT^{4+} ring between the TTF and DNP sites in bistable [2]rotaxanes **2a** and **2b**, with the TTF unit being neutral (states A and B) or oxidized to TTF$^{+\bullet}$ or TTF^{2+} (states C and D).

CBPQT^{4+} ring encircling the DNP site to form the less stable MSCC.[17] For foldamer-incorporated bistable [2]rotaxanes **2a** and **2b**, the barrier energy for the shuttling of CBPQT^{4+} should be substantially increased due to the hindrance of the foldamer segment. The ^{1}H NMR spectra of [2]rotaxanes **2a** (Fig. 5d) and **2b** in acetonitrile-d_3 and acetone-d_6 displayed one set of signals, suggesting that the CBPQT^{4+} ring either shuttled rapidly between the TTF and DNP sites (A↔B, Fig. 6) or predominantly existed in the GSCC (A, Fig. 6). Since the above kinetic investigation (Table 2) revealed that the slipping rates of the CBPQT^{4+} ring over the dimeric (**1b**) and trimeric (**1c**) foldamer segments were slow on the ^{1}H NMR time scale, it was reasonable to propose that the GSCC was formed predominantly.Considering the TTF sides of their threads possess the same structure, the rate constant of the shuttling of the CBPQT^{4+} ring in [2]rotaxanes **2a** and **2b** from their GSCC to the MSCC should be similar to the corresponding rate constant of decomplexation of pseudo[2]rotaxanes **1b** and **1c** in the same solvent. Upon oxidation of the TTF unit to TTF$^{+\bullet}$ or TTF^{2+}, the CBPQT^{4+} ring of the [2]rotaxanes would be repelled to slip more rapidly over the foldamer segment to encircle the DNP unit (C→D, Fig. 6), and the shuttling rates should be comparable to the rates of decomplexation of the corresponding oxidized pseudo-[2]rotaxanes **1b** and **1c** in the same solvent (Table 4). Reduction of the TTF$^{+\bullet}$ or TTF^{2+} cation of the [2]rotaxanes to TTF would lead to the formation of the MSCC (B, Fig. 6), and the CBPQT^{4+} ring would slip back to the TTF side to form the GSCC (B→A, Fig. 6). The last process is directly related to the lifetime of the MSCC and is critical for non-volatile molecular memory with high metastability.

To get more insight into this last process, the CVs of the two bistable [2]rotaxanes at varying scan rates in both acetonitrile and chloroform were recorded. For the second scans, for **2a** in acetonitrile, at the slow scan rates of 5 and 10 mV/s, no peak was observed at about 0.44 V, which is typical for the free TTF and, for bistable [2]rotaxane **2a**, associated with its MSCC. Within the range of scan rates from 25 mV/s to 75 mV/s, this peak was observed and intensified pronouncedly. This result indicates that even in solution the MSCC of **2a** had a relatively long lifetime at ambient temperature, which is comparable with that observed in CBPQT^{4+}–TTF–DNP-based rotaxanes entrapped in the solid-state polymer.[17b] With the further increase of the scan rate from 100 mV/s to 400 mV/s, this peak still survived, but became weakened, which might be attributed to the decreased C→D conversion (Fig. 6) at increased scan rates. For **2a** in chloroform and **2b** in both chloroform and acetonitrile, no peaks corresponding to the free TTF unit were observed at different scan rates, which might reflect the decreased C→D conversion as well as the increased stability of the MSCC of the [2]rotaxanes.

The ^{1}H NMR spectra in CD_3CN showed that adding 2.0 equiv of Magic Blue to the solution of the [2]rotaxanes resulted in the appearance of a new set of signals. For **2a**, the two signals (at 5.78 and 5.89 ppm) of the protons of the TTF unit encapsulated in the CBPQT^{4+} ring disappeared (Fig. 5d), while the signals of the H2/6 (at 6.16 and 6.20 ppm) and H3/7 (at 5.89 ppm) protons of the DNP unit encapsulated in the CBPQT^{4+} ring emerged (see structure in Chart 1 for numbering) (Fig. 5e).[29] These results supported that the CBPQT^{4+} ring had shuttled from the TTF side to the DNP side. In separate UV–vis experiments, both **2a** and **2b** were oxidized with 2.0 equiv of $Fe(ClO_4)_3$ in acetonitrile to produce doubly oxidized TTF^{2+}. After standing for 50 min, the solutions were quickly treated with an excess of zinc powder to reduce TTF^{2+} to TTF. The time-dependent UV–vis spectra of the solutions were then recorded, which showed that the DNP–CBPQT^{4+} CT absorption gradually decreased, while the TTF–CBPQT^{4+} CT absorption formed and increased (Fig. 7). By assuming a first-order kinetics, we determined the rate constants of the shuttling of the CBPQT^{4+} ring of **2a** and **2b** from the MSCC to the GSCC to be 1.1×10^{-2} and 7.4×10^{-4} s^{-1}, respectively, which corresponded to half-lives of 66 and 930 s. Using

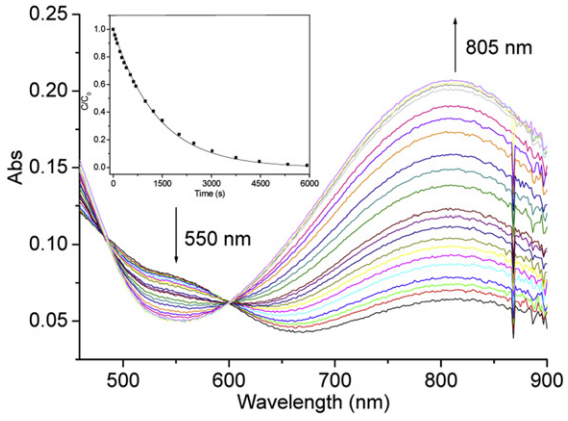

Fig. 7. The UV–vis absorption spectra of the solution of bistable [2]rotaxane **2b** in acetonitrile at 25 °C, obtained after zinc powder (5 equiv) was added to the solution of its dioxidized sample. Inset: The plot of C/C_0 versus the recording time (from 160 s to 12,300 s).

the same method, the rate constant of the same process of **2a** in chloroform was determined to be 9.9×10^{-6} s^{-1}, which corresponded to a half-life of 19.5 h, 1064 times longer than that in acetonitrile. The rate constants were all higher than the related k_{off} values of pseudo[2]rotaxanes **1b** and **1c** (Table 2), which was consistent with the fact that the donor–acceptor interaction between DNP and $CBPQT^{4+}$ was weaker than that between TTF and $CBPQT^{4+}$. Since the foldamer segments were not symmetric, the energy barrier experienced by $CBPQT^{4+}$ ring from the two sides might be slightly different, which should also contribute to the difference. Remarkably, the solution of the MSCC of **2b** in chloroform, obtained using the similar method, did not exhibit a perceptible TTF–$CBPQT^{4+}$ CT band in the UV–vis spectrum even after 3 days, indicating that the foldamer segment can efficiently block the conversion of MSCC to GSCC in less polar media.

3. Conclusion

We have demonstrated that hydrogen bonding-induced arylamide foldamers can serve as deformable moiety in switchable pseudorotaxanes and rotaxanes to modulate the switching kinetics and metastability. The noncovalent nature of the folding conformation in foldamers endows structural flexibility, making the foldamers versatile structural units to modulate the mechanical movements of the $CBPQT^{4+}$ ring along the dumbbell component. By varying the number of the repeating units in the foldamer, the kinetics of the solvent-dependent slippage/deslippage process of pseudo-[2]rotaxanes can be tuned to cover a large span of more than 7.0×10^5 times. Changing the oxidative state of the TTF unit significantly increases the rate of the $CBPQT^{4+}$ ring extruding off the dumbbell. In bistable [2]rotaxanes where foldamer segments are introduced to bridge a TTF unit and a DNP unit in the dumbbell, the deformable sizes of the foldamers effectively serve as a steric barrier to the relaxation from MSCC to GSCC. The lifetime of the post-oxidation MSCC is thus dramatically increased. As shown in the case for one [2]rotaxane in its metastable state in chloroform, no relaxation to the ground state is observed even after 3 days! The generation of such a long-lived MSCC in [2]rotaxanes holds great promises for the application of these mechanically interlocked molecules in non-volatile molecular memories.

The marriage of deformable foldamers and interlocked molecular switches opens up the possibility of exploring more responsive dynamic molecular materials. In principle, many other folding patterns could be used for the similar purpose. The diversity of folding patterns enables the future design of foldamer stoppers that can operate in medium of discrete polarity or be modulated chemically, photochemically or by molecular recognition.[35–37] Because the foldamers tune the slippage of the ring through changing their shape or conformation, which only involves the breaking of noncovalent bonds, it is expected that longer foldamer segments can be utilized to further increase the metastability, without completely blocking the slippage of a properly sized ring over them. Hence, this family of soft deformable foldamers also avoids the all-or-nothing character displayed by most of the conventional stoppers.

4. Experimental section

4.1. General methods

All reagents and chemicals were obtained from commercial sources and used without further purification unless otherwise noted. The solvents have been purified by standard procedures before use. The ^1H and ^{13}C NMR spectra were recorded on Varian Mercury 300 or 400 MHz spectrometers in the indicated solvents. Chemical shifts are expressed in parts per million (δ) using residual proton resonances of the deuterated solvents as the internal standards. UV–vis spectra were recorded on a CARY 100 spectrometer; Cyclic voltammetric measurements were carried out in a three-electrode cell using a Pt button working electrode of 2 mm diameter, a Pt wire counter electrode, and an Ag/AgCl reference electrode on a computer-controlled CHI610D instrument. The synthesis and characterization of compounds **7**–**11**, **13**, **3b**, and **3c**, pseudorotaxanes **1b** and **1c**, compounds **18**, **19**, **21**, **22**, **24a**, and **24b** have been described.[19]

*4.1.1. Compound **3d**.* A suspension of **14** (0.15 g, 0.070 mmol) and $LiOH\cdot H_2O$ (0.16 g, 3.68 mmol) in THF (4 mL) and water (1 mL) was stirred for 18 h and then acidified with aqueous HCl. The solvent was removed and the resulting slurry triturated with CH_2Cl_2 (30 mL). The organic phase was successively washed with water (30×2 mL) and brine (30 mL), dried over anhydrous Na_2SO_4, and concentrated to give **15** as a yellow oil (0.15 g, 100%). Without further purification, this acid was dissolved in CH_2Cl_2 (2 mL). To the solution were added NMM (11.4 μL, 0.092 mmol) and $ClCO_2Et$ (10.0 μL, 0.076 mmol). After stirring for 1 h, a solution of **16d**[23b] (88 mg, 0.14 mmol) in CH_2Cl_2 (1 mL) was added and stirring was continued for another 5 h. The solution was successively washed with water (30 mL×2) and brine (30 mL), dried over anhydrous Na_2SO_4, and concentrated. The resulting residue was subject to column chromatography ($CHCl_3$) to give **3b** as a pale yellow oil (102 mg, 52%). Pale yellow solid. ^1H NMR (400 MHz, $CDCl_3$) δ: 10.10 (s, 1H), 9.88 (s, 1H), 9.83 (s, 1H), 8.96 (s, 1H), 8.78–8.89 (m, 3H), 8.46 (dd, J_1=8.2 Hz, J_2=1.2 Hz, 1H), 7.82–7.80 (m, 3H), 7.54 (dd, J_1=6.4 Hz, J_2=1.6 Hz, 1H), 7.35–3.32 (m, 44H), 6.60–6.58 (m, 12H), 6.52 (d, J=2.0 Hz, 2H), 6.48 (t, J=2.0 Hz, 4H), 6.46 (br, 3H), 6.24 (d, J=1.2 Hz, 1H), 6.20 (s, 1H), 4.94 (s, 16H), 4.88 (br, 12H), 4.41 (s, 2H), 4.16 (s, 2H), 3.93 (s, 3H), 3.90 (s, 6H), 3.85 (s, 3H), 3.84 (s, 3H), 3.77–3.75 (m, 2H), 3.66–3.64 (m, 2H), 3.48–3.58 (m, 20H), 2.79 (t, J=6.4 Hz, 2H), 2.73–2.71 (m, 2H). ^{13}C NMR (100 MHz, $CDCl_3$) δ: 168.31, 165.78, 163.30, 163.24, 163.06, 160.24, 160.15, 160.07, 149.38, 147.78, 147.52, 147.41, 140.98, 139.45, 139.34, 136.89, 133.22, 132.43, 132.38, 131.34, 128.65, 128.06, 127.63, 126.70, 126.67, 126.49, 126.44, 126.39, 126.26, 125.90, 125.86, 125.76, 125.49, 125.07, 124.83, 124.55, 123.51, 123.07, 122.96, 122.93, 122.89, 112.43, 111.84, 111.80, 106.69, 106.55, 106.48, 101.68, 101.32, 73.13, 71.25, 71.05, 70.71, 70.59, 70.53, 70.44, 70.15, 70.05, 69.73, 69.66, 69.56, 63.14, 62.71, 62.54, 52.37, 35.23. MS (MALDI-TOF) m/z: 2819.2 $[M+H]^+$. HRMS (MALDI-TOF): calcd for $C_{160}H_{154}N_4O_{31}S_6$ $[M]^+$: 2818.8921. Found: 2818.8900.

*4.1.2. Compound **3a**.* Pale yellow solid. ^1H NMR (400 MHz, $CDCl_3$) δ: 9.16 (s, 2H), 8.60 (d, J=8.0 Hz, 1H), 7.59 (d, J=8.0 Hz, 1H), 7.43–7.31 (m, 40H), 7.18 (t, J=8.0 Hz, 1H), 6.70–6.69 (m, 12H), 6.62–6.61 (m, 2H), 6.59–6.58 (m, 4H), 6.57–6.56 (m, 3H), 6.37–6.36 (m, 2H), 5.04 (s, 16H), 4.98 (s, 12H), 4.51 (s, 2H), 3.94 (s, 3H), 3.90 (s, 3H), 3.80–3.78 (m, 2H), 3.75–3.73 (m, 2H), 3.66–3.61 (m, 20H), 2.93–2.89 (m, 4H). ^{13}C NMR (100 MHz, $CDCl_3$) δ: 168.2, 165.9, 160.3, 160.2, 160.1, 149.4, 141.1, 139.5, 139.4, 136.9, 132.3, 128.7, 128.1, 127.7, 126.7 (d), 126.3, 124.5, 124.4, 123.9, 123.0 (d), 122.9, 112.4, 112.3, 112.2, 112.1, 106.7, 106.6, 106.5, 101.7 (d), 101.4, 73.2, 71.4, 71.1, 70.8 (d), 70.7, 70.6 (d), 70.2, 70.1, 69.8, 69.7, 69.6, 62.3, 52.4, 35.3. MS (MALDI-TOF) m/z: 2371.8 $[M]^+$. HRMS (MALDI-TOF): calcd for $C_{136}H_{133}NO_{25}S_6$ $[M]^+$: 2373.7491. Found: 2373.7460.

*4.1.3. Pseudorotaxane **1d**.* A solution of **3d** (29 mg, 0.01 mmol) and $CBPQT\cdot 4PF_6$ (11 mg, 0.01 mmol) in acetone (0.25 mL) and acetonitrile (0.25 mL) was stirred for 36 h and then concentrated. The resulting green solid was dissolved in acetonitrile (10 mL) and to the solution added water (40 mL) quickly. The formed dark green solid was filtrated and washed with aqueous acetonitrile (20%, 20 mL×4) and ether (10 mL). The solid was then triturated with

CH_2Cl_2 (15 mL) and the insoluble solid was removed by filtration, which was CBPQT·$4PF_6$ as evidenced by ^{1}H NMR. The solution was again concentrated and the resulting residue triturated successively with a mixture of CH_2Cl_2 and PE (1:2, 10 mL×4) to remove free **3d**. The solid was then dried in vacuo to give pure **1d** as a green solid (21 mg, 53%). ^{1}H NMR (400 MHz, CD_3CN) δ: 10.09 (s, 1H), 9.92 (br, 2H), 8.87 (d, J=6.0 Hz, 8H), 8.82 (s, 1H), 8.67 (d, J=8.0 Hz, 1H), 8.59 (br, 2H), 8.31 (d, J=8.0 Hz, 1H), 7.83 (br, 8H), 7.74–7.69 (m, 3H), 7.54 (s, 8H), 7.50–7.46 (m, 1H), 7.42–7.39 (m, 1H), 7.33–7.15 (m, 43H), 6.59–6.56 (m, 8H), 6.54–6.53 (m, 4H), 6.49–6.44 (m, 6H), 6.41–6.36 (m, 3H), 5.93 (d, J=13 Hz, 1H), 5.82 (d, J=17 Hz, 1H), 5.60–5.53 (m, 8H), 4.96–4.93 (m, 16H), 4.89–4.84 (m, 12H), 4.25 (s, 2H), 4.08–4.50 (m, 2H), 3.93 (s, 3H), 3.90–3.86 (m, 6H), 3.81–3.80 (m, 6H), 3.71–3.61 (m, 16H), 3.57 (br, 2H), 3.50 (br, 2H), 3.48–3.40 (m, 4H), 2.96–2.90 (m, 4H). MS (ESI) m/z: 835.54 $[M-4PF_6]^{4+}$, 1162.04 $[M-3PF_6]^{3+}$, $[M-2PF_6]^{2+}$ 1185.54. HRMS (ESI): calcd for $C_{196}H_{186}F_{12}N_8O_{31}P_2S_6$ $[M-2PF_6]^{2+}$: 1814.5416]. Found: 1814.5417.

*4.1.4. Bistable [2]rotaxane **2a** and thread **4a**.* A suspension of **24a** (35 mg, 0.033 mmol) and Pd/C (10%, 30 mg) in THF (5 mL) was stirred at 40 °C under the atmosphere of hydrogen for 30 h and then cooled. The solid was removed by filtration and the filtrate concentrated to give **25a** as a sticky oil (33 mg, 96%). Without further purification, this amine was dissolved in chloroform (1 mL) for the next step. To a solution of **15** (70 mg, 0.033 mmol) in chloroform (2 mL) were added NMM (5.3 μL, 0.043 mmol) and $ClCO_2Et$ (4.7 μL, 0.039 mmol). The solution was stirred for 1 h and then concentrated. The resulting slurry was dissolved in THF (2 mL) and the insoluble residue removed by filtration. The filtrate was concentrated again and the resulting orange oil dissolved in acetone (0.6 mL) and acetonitrile (0.3 mL). CBPQT·$4PF_6$ (34 mg, 0.031 mmol) and the above solution of **25a** were added and the mixture stirred for 24 h and then concentrated to afford a dark green solid. The residue was supersonicated in CH_2Cl_2 (12 mL) and PE (18 mL) for 2 h and then insoluble green residue removed by filtration. The resulting green solid was dissolved in acetonitrile (10 mL). Water (40 mL) was added dropwise and the formed precipitate filtrated out again and washed with acetonitrile and water (100 mL, 1:4) thoroughly. The solid was dissolved in a solution of NH_4PF_6 (0.10 g) in acetone (5 mL) and the solution was concentrated. The resulting slurry was triturated with water (10 mL). The insoluble green residue was filtrated out again, washed with water (10 mL×3) and ether (5 mL) and dried in vacuo to afford **2a** as a green solid (24 mg, 18%). The filtrate of CH_2Cl_2 and PE was concentrated with a rotavapor and the resulting residue subjected to column chromatography (n-hexane/chloroform 1:1) to give **4a** as an orange solid foam (40 mg, 40%). [2]*Rotaxane* **2a**. ^{1}H NMR (400 MHz, CD_3COCD_3) δ: 10.05 (s, 1H), 9.31 (br, 8H), 8.90 (s, 1H), 8.45 (d, J=7.6 Hz, 1H), 8.32–8.15 (m, 9H), 7.77 (s, 8H), 7.70–7.60 (m, 4H), 7.31–7.10 (m, 44H), 7.04 (t, J=8.4 Hz, 1H), 6.98–6.90 (m, 3H), 6.83–6.77 (m, 2H), 6.60 (s, 8H), 6.56 (s, 4H), 6.49 (br, 6H), 6.43 (br, 1H), 6.33 (s, 2H), 6.06 (d, J=12.8 Hz, 1H), 5.96 (d, J=13.6 Hz, 1H), 5.85 (br, 8H), 4.93 (s, 16H), 4.89 (s, 8H), 4.84 (s, 4H), 4.20 (s, 2H), 4.08 (t, J=6.0 Hz, 2H), 4.05 (s, 2H), 3.99 (t, J=6.0 Hz, 2H), 3.83–3.81 (m, 6H), 3.75–3.66 (m, 12H), 3.63 (s, 4H), 3.57–3.55 (m, 2H), 3.50–3.48 (m, 2H), 3.44–3.37 (m, 6H), 3.32–3.29 (m, 2H), 3.24–3.20 (m, 2H), 3.05–3.00 (m, 2H), 2.99–2.94 (m, 2H), 1.87–1.68 (m, 8H), 1.54–1.49 (m, 2H), 1.46–1.40 (m, 2H), 1.32–1.16 (m, 14H), 1.06 (d, J=6.8 Hz, 12H). ^{13}C NMR (100 MHz, CD_3COCD_3) δ: 167.8, 165.4, 162.1, 159.7, 159.6, 159.4, 154.1, 153.0, 147.4, 146.6, 145.4, 144.3, 141.1, 140.7, 139.3, 136.8, 135.9, 131.7, 131.1, 130.5, 128.5, 127.9, 127.7, 127.3, 127.1, 126.3 (d), 126.0, 125.9, 125.5, 124.7 (d), 124.5, 124.3, 124.0, 123.9, 123.5, 123.3, 122.0, 119.7, 119.6, 119.3, 119.0, 113.4, 113.2, 108.3, 108.2, 107.9 (d), 106.0, 104.9 (d), 100.6, 100.2, 74.0, 71.6, 70.4, 70.0, 69.9, 69.8, 69.6 (d), 69.5, 69.4 (d), 69.2, 69.0, 68.9, 69.8 (d), 67.4, 64.2, 61.8, 61.4, 39.1, 34.7, 34.3, 29.6, 26.4, 25.7, 25.6, 23.0, 22.4. MS (ESI): 900.12 $[M-4PF_6]^{4+}$, 1249.05 $[M-3PF_6]^{3+}$. HRMS (ESI): calcd for $C_{218}H_{227}N_7O_{29}S_6$ $[M-4PF_6]^{4+}$: 899.6207. Found: 899.6200. *Thread* **4a**. ^{1}H NMR (400 MHz, $CDCl_3$) δ: 10.03 (s, 1H), 9.00 (s, 1H), 8.71 (d, J=8.0 Hz, 1H), 8.51 (d, J=8.0 Hz, 1H), 7.90–7.84 (m, 3H), 7.69 (d, J=8.0 Hz, 1H), 7.40–7.29 (m, 44H), 7.09 (s, 3H), 6.83 (t, J=8.4 Hz, 2H), 6.67 (s, 12H), 6.60 (s, 2H), 6.56 (s, 4H), 6.53 (s, 3H), 6.31 (s, 1H), 6.30 (s, 1H), 5.00 (s, 16H), 4.95 (s, 12H), 4.49 (s, 2H), 4.20 (s, 2H), 4.17 (t, J=6.0 Hz, 2H), 4.10 (t, J=5.6 Hz, 2H), 3.92 (s, 3H), 3.85 (s, 3H), 3.82–3.79 (m, 4H), 3.74 (br, 2H), 3.66–3.54 (m, 20H), 3.49–3.45 (m, 2H), 3.35–3.31 (m, 2H), 2.88–2.84 (m, 4H), 2.03–1.89 (m, 6H), 1.83–1.80 (m, 2H), 1.63–1.62 (m, 2H), 1.54–1.52 (m, 2H), 1.44–1.26 (m, 14H), 1.23 (d, J=7.2 Hz, 12H). ^{13}C NMR (100 MHz, $CDCl_3$) δ: 168.2, 165.3, 163.0, 160.2, 160.1, 160.0, 154.7 (d), 153.4, 147.4, 147.1, 141.9, 140.9, 139.4, 139.3, 136.8, 132.1, 131.2, 128.6, 128.1, 127.6, 127.2, 126.8 (d), 126.6 (d), 126.5, 126.4, 125.9, 125.7, 125.4, 125.2, 125.1, 124.5, 124.0, 123.9, 123.1, 123.0 (d), 122.9, 114.2, 114.1, 112.5, 111.8, 106.6, 106.5, 106.4, 105.3, 101.6, 101.5, 101.2, 74.8, 73.1, 71.2, 71.0, 70.7 (d), 70.6, 70.5, 70.1, 70.0, 69.8, 69.6, 69.5. 68.2, 68.0, 62.7, 62.5, 40.0, 35.2, 30.4, 29.8, 29.7, 29.5, 29.4 (d), 27.2, 26.5, 26.3, 24.2, 23.1. MS (MALDI-TOF) m/z: 3078.2 $[M]^+$. HRMS (MALDI-TOF): calcd for $C_{182}H_{195}N_3O_{29}S_6$: 3078.2201 $[M]^+$. Found: 3078.2228.

*4.1.5. Bistable [2]rotaxane **2b**.* Green solid. ^{1}H NMR (400 MHz, CD_3COCD_3) δ: 10.08 (s, 1H), 10.04 (s, 1H), 9.35 (br, 8H), 8.96 (s, 1H), 8.54–8.52 (m, 1H), 8.48 (d, J=6.8 Hz, 1H), 8.31–8.25 (m, 9H), 7.78 (br, 8H), 7.70–7.62 (m, 5H), 7.31–7.14 (m, 45H), 7.07 (t, J=8.0 Hz, 1H), 6.98–6.90 (m, 3H), 6.83–6.76 (m, 2H), 6.60 (br, 8H), 6.56 (s, 4H), 6.50 (br, 6H), 6.44 (s, 1H), 6.31 (s, 2H), 6.09 (d, J=13.6 Hz, 1H), 6.01 (d, J=13.6 Hz, 1H), 5.87 (s, 8H), 4.94 (s, 16H), 4.90 (s, 8H), 4.85 (s, 4H), 4.19 (s, 2H), 4.09 (t, J=6.0 Hz, 2H), 4.06 (s, 2H), 4.00 (d, J=6.0 Hz, 2H), 3.91 (br, 6H), 3.82 (s, 3H), 3.73–3.66 (m, 14H), 3.62 (s, 4H), 3.58–3.52 (m, 2H), 3.50–3.46 (m, 2H), 3.43–3.35 (m, 6H), 3.30–3.27 (m, 2H), 3.26–3.19 (m, 2H), 3.02–2.95 (m, 4H), 1.85–1.70 (m, 8H), 1.53–1.50 (m, 2H), 1.43–1.40 (m, 2H), 1.30–1.15 (m, 14H), 1.06 (d, J=6.8 Hz, 12H). ^{13}C NMR (100 MHz, CD_3COCD_3) δ: 167.8, 165.2, 162.7, 162.4, 159.7, 159.6, 159.4, 154.1, 153.1, 147.5, 147.4, 146.7, 145.5, 145.4, 144.3, 141.1, 140.7, 139.3, 136.8, 135.9 (d), 132.1, 131.8, 131.1, 131.0, 130.5, 128.6, 127.9, 127.7, 127.3, 127.1, 126.7, 126.6, 126.3, 125.5, 125.4, 125.3, 124.7 (d), 124.5, 124.4, 124.1, 123.9, 123.8, 123.7, 123.3, 122.1, 119.8, 119.6, 119.3, 119.0, 118.7, 113.4, 113.3, 108.4, 108.3 (d), 107.9, 106.0, 104.9 (d), 100.6, 100.2, 74.0, 71.6, 70.4, 70.0, 69.8, 69.7, 69.5 (d), 69.4, 69.2, 69.0, 68.9, 68.8, 67.4, 64.2, 62.3, 61.9, 61.4, 39.1, 34.7, 34.3, 29.6, 26.4, 25.7, 25.6, 23.0, 22.4. HRMS (ESI): calcd for $C_{226}H_{234}N_8O_{31}S_6$ $[M-4PF_6]^4$: 936.8826. Found: 936.8671. HRMS (ESI): calcd for $C_{226}H_{234}F_6N_8O_{31}PS_6$ $[M-3PF_6]^{3+}$: 1297.4984. Found: 1297.4784. *Thread* **4b**. Orange solid in 15% yield. ^{1}H NMR ($CDCl_3$, 400 MHz) δ: 9.86 (s, 1H), 9.78 (s, 1H), 8.92 (s, 1H), 8.70 (d, J=8.0 Hz, 1H), 8.63 (d, J=7.6 Hz, 1H), 8.44 (d, J=7.6 Hz, 1H), 7.82–7.50 (m, 4H), 7.59 (d, J=7.6 Hz, 1H), 7.38–7.18 (m, 46H), 7.08 (t, J=6.0 Hz, 1H), 7.02 (br, 3H), 6.79–6.72 (m, 2H), 6.59 (br, 12H), 6.51 (br, 2H), 6.48 (br, 4H), 6.45 (br, 3H), 6.24 (d, J=2.0 Hz, 1H), 6.20 (s, 1H), 4.93 (s, 16H), 4.88 (br, 12H), 4.41 (s, 2H), 4.15 (s, 2H), 4.10 (t, J=6.0 Hz, 2H), 4.03 (t, J=6.0 Hz, 2H), 3.89 (s, 3H), 3.88 (s, 3H), 3.79 (s, 3H), 3.78–3.65 (m, 6H), 3.60–3.45 (m, 20H), 3.44–3.38 (m, 2H), 3.29–3.23 (m, 2H), 2.82–2.70 (m, 4H), 2.00–1.70 (m, 8H), 1.60–1.42 (m, 4H), 1.35–1.70 (m, 14H), 1.15 (d, J=6.8 Hz, 12H). ^{13}C NMR (DMSO-d_6, 100 MHz) δ: 168.3, 165.7, 163.4, 162.9, 159.5, 159.4, 159.3, 153.9, 152.9, 148.5, 147.9, 147.1, 141.1, 140.9, 139.3, 139.2, 136.8, 131.8, 131.5, 131.1, 130.1, 128.3, 128.1, 127.8, 127.7, 127.6, 127.2, 125.9, 125.8 (d), 125.3, 125.2 (d), 124.8, 124.5, 124.3, 124.2, 123.7, 123.6, 123.1 (d), 122.6, 113.3 (d), 111.0 (d), 110.9 (d), 106.4, 106.1, 105.6, 105.5, 101.0, 100.7, 74.2, 71.7, 70.4, 70.0, 69.7, 69.6 (d), 69.5, 69.2, 69.0 (d), 68.7, 68.6, 67.6, 62.6, 62.1, 61.7, 34.6, 30.2, 29.6, 28.9 (d), 28.7, 28.5 (d), 26.4, 25.7, 25.6, 23.8, 22.5. MS (MALDI-TOF) m/z:

3227.3 $[M]^+$. HRMS (MALDI-TOF): calcd for $C_{190}H_{202}N_4O_{31}S_6$ $[M]^+$: 3227.2677. Found: 3227.2652.

Acknowledgements

We thank NSFC (20732007, 20921091, 20872167, 20974118), and STCSM (10PJ1412200 and 09XD1405300) for financial support.

References and notes

1. (a) Schill, G. *Catenanes, Rotaxanes, and Knots*; Academic: New York, NY, 1971; 192; (b) *Molecular Catenanes, Rotaxanes and Knots: a Journey through the World of Molecular Topology*; Sauvage, J.-P., Dietrich-Buchecker, C., Eds.; Wiley-VCH: Weinheim, 1999; p 368.
2. (a) Amabilino, D. B.; Stoddart, J. F. *Chem. Rev.* **1995**, *95*, 2725–2828; (b) Sauvage, J.-P. *Acc. Chem. Res.* **1998**, *31*, 611–619.
3. (a) Glink, P. T.; Schiavo, C.; Stoddart, J. F.; Williams, D. J. *Chem. Commun.* **1996**, 1483–1490; (b) Harada, A.; Hashidzume, A.; Yamaguchi, H.; Takashima, Y. *Chem. Rev.* **2009**, *109*, 5974–6023.
4. (a) Crowley, J. D.; Goldup, S. M.; Lee, A.-L.; Leigh, D. A.; McBurney, R. T. *Chem. Soc. Rev.* **2009**, *38*, 1530–1541; (b) Silvi, S.; Venturi, M.; Credi, A. *J. Mater. Chem.* **2009**, *19*, 2279–2294; (c) Stoddart, J. F. *Chem. Soc. Rev.* **2009**, *38*, 1802–1820; (d) Durot, S.; Reviriego, F.; Sauvage, J.-P. *Dalton Trans.* **2010**, *39*, 10557–10570.
5. (a) Bissell, R. A.; Córdova, E.; Kaifer, A. E.; Stoddart, J. F. *Nature* **1994**, *369*, 133–137; (b) Altieri, A.; Gatti, F. G.; Kay, E. R.; Leigh, D. A.; Martel, D.; Paolucci, F.; Slawin, A. M. Z.; Wong, J. K. Y. *J. Am. Chem. Soc.* **2003**, *125*, 8644–8654; (c) Collin, J. P.; Gavina, P.; Heitz, V.; Sauvage, J.-P. *Eur. J. Inorg. Chem.* **1998**, 1–14.
6. (a) Balzani, V.; Gómez-López, M.; Stoddart, J. F. *Acc. Chem. Res.* **1998**, *31*, 405–414; (b) Harada, A. *Acc. Chem. Res.* **2001**, *34*, 456–464; (c) Kay, E. R.; Leigh, D. A. *Top. Curr. Chem.* **2005**, *262*, 133–177; (d) Tian, H.; Wang, Q.-C. *Chem. Soc. Rev.* **2006**, *35*, 361–374; (e) Balzani, V.; Credi, A.; Venturi, M. *Chem. Soc. Rev.* **2009**, *38*, 1542–1550.
7. (a) Pease, A. R.; Jeppesen, J. O.; Stoddart, J. F.; Luo, Y.; Collier, C. P.; Heath, J. R. *Acc. Chem. Res.* **2001**, *34*, 433–444; (b) Trabolsi, A.; Fahrenbach, A. C.; Dey, S. K.; Share, A. I.; Friedman, D. C.; Basu, S.; Gasa, T. B.; Khashab, N. M.; Saha, S.; Aprahamian, I.; Khatib, H. A.; Flood, A. H.; Stoddart, J. F. *Chem. Commun.* **2010**, 871–873.
8. (a) Flood, A. H.; Stoddart, J. F.; Steuerman, D. W.; Heath, J. R. *Science* **2004**, *306*, 2055–2056; (b) Choi, J. W.; Flood, A. H.; Steuerman, D. W.; Nygaard, S.; Braunschweig, A. B.; Moonen, N. N. P.; Laursen, B. W.; Luo, Y.; Delonno, E.; Peters, A. J.; Jeppesen, J. O.; Xe, K.; Stoddart, J. F.; Heath, J. R. *Chem.—Eur. J.* **2006**, *12*, 261–279.
9. Li, H.; Zhao, Y.-L.; Fahrenbach, A. C.; Kim, S.-Y.; Paxton, W. F.; Stoddart, J. F. *Org. Biomol. Chem.* **2011**, *9*, 2240–2250.
10. *Foldamers: Structure, Properties and Applications*; Hecht, S., Huc, I., Eds.; Wiley-VCH: Weinheim, 2007; p 456.
11. (a) Gong, B. *Chem.—Eur. J.* **2001**, *7*, 4336–4342; (b) Huc, I. *Eur. J. Org. Chem.* **2004**, 17–29; (c) Gong, B. *Acc. Chem. Res.* **2008**, *41*, 1376–1386; (d) Saraogi, I.; Hamilton, A. D. *Chem. Soc. Rev.* **2009**, *38*, 1726–1743; (e) Guichard, G.; Ivan Huc, I. *Chem. Commun.* **2011**, 5933–5941.
12. (a) Li, Z.-T.; Hou, J.-L.; Li, C.; Yi, H.-P. *Chem.—Asian J.* **2006**, *1*, 766–778; (b) Li, Z.-T.; Hou, J.-L.; Li, C. *Acc. Chem. Res.* **2008**, *41*, 1343–1353; (c) Zhao, X.; Li, Z.-T. *Chem. Commun.* **2010**, 1601–1616.
13. Shi, Z.-M.; Huang, J.; Ma, Z.; Guan, Z.; Li, Z.-T. *Macromolecules* **2010**, *43*, 6185–6192.
14. Philp, D.; Slawin, A. M. Z.; Spencer, N.; Stoddart, J. F.; Williams, D. J. *J. Chem. Soc., Chem. Commun.* **1991**, 1584–1586.
15. Li, Z.-T.; Stein, P. C.; Svenstrup, N.; Lund, K. H.; Becher, J. *Angew. Chem., Int. Ed. Engl.* **1995**, *34*, 2524–2528.
16. A pseudorotaxane consisting of a MeS-bearing TTF-DNP thread and a $CBPQT^{4+}$ ring had been reported to have a rotaxane-like character, see: Jeppesen, J. O.; Becher, J.; Stoddart, J. F. *Org. Lett.* **2002**, *4*, 557–560.
17. For examples, of bistable rotaxanes based on the $CBPQT^{4+}$ ring and TTF and DNP-containing dumbbell component, see: (a) Jeppesen, J. O.; Perkins, J.; Becher, J.; Stoddart, J. F. *Angew. Chem., Int. Ed.* **2001**, *40*, 1216–1221; (b) Steuerman, D. W.; Tseng, H.-R.; Peters, A. J.; Flood, A. H.; Jeppesen, J. O.; Nielsen, K. A.; Stoddart, J. F.; Heath, J. R. *Angew. Chem., Int. Ed.* **2004**, *43*, 6486–6491; (c) Flood, A. H.; Peters, A. J.; Vignon, S. A.; Steuerman, D. W.; Tseng, H.-R.; Kang, S.; Heath, J. R.; Stoddart, J. F. *Chem.—Eur. J.* **2004**, *10*, 6558–6564.
18. For examples, of controllable shuttling of rotaxanes, see (a) Kang, S.; Vignon, S. A.; Tseng, H. R.; Stoddart, J. F. *Chem.—Eur. J.* **2004**, *10*, 2555–2564; (b) Nygaard, S.; Laursen, B. W.; Flood, A. H.; Hansen, C. N.; Jeppesen, J. O.; Stoddart, J. F. *Chem. Commun.* **2006**, 144–146; (c) Jeppesen, J. O.; Nygaard, S.; Vignon, S. A.; Stoddart, J. F. *Eur. J. Org. Chem.* **2005**, 196–220; (d) Alvarez-Pérez, M.; Goldup, S. M.; Leigh, D. A.; Slawin, A. M. Z. *J. Am. Chem. Soc.* **2008**, *130*, 1836–1838.
19. A preliminary communication has been reported, see: Zhang, K.-D.; Zhao, X.; Wang, G.-T.; Liu, Y.; Zhang, Y.; Lu, H.-J.; Jiang, X.-K.; Li, Z.-T. *Angew. Chem., Int. Ed.* **2011**, *50*, 9866–9870.
20. Hawker, C. J.; Fréchet, M. J. *J. Am. Chem. Soc.* **1990**, *112*, 7638–7647.
21. Amabilino, D. B.; Ashton, P. R.; Balzani, V.; Brown, C. L.; Credi, A.; Fréchet, J. M. J.; Leon, J. W.; Raymo, F. M.; Spencer, N.; Stoddart, J. F.; Venturi, M. *J. Am. Chem. Soc.* **1996**, *118*, 12012–12020.
22. (a) Hou, J.-L.; Yi, H.-P.; Shao, X.-B.; Li, C.; Wu, Z.-Q.; Jiang, X.-K.; Wu, L.-Z.; Tung, C.-H.; Li, Z.-T. *Angew. Chem., Int. Ed.* **2006**, *45*, 796–800; (b) Yi, H.-P.; Wu, J.; Ding, K.-L.; Jiang, X.-K.; Li, Z.-T. *J. Org. Chem.* **2007**, *72*, 870–877.
23. (a) Qin, B.; Chen, X. Y.; Fang, X.; Shu, Y. Y.; Yip, Y. K.; Yan, Y.; Pan, S. Y.; Ong, W. Q.; Ren, C. L.; Su, H. B.; Zeng, H. Q. *Org. Lett.* **2008**, *10*, 5127–5130; (b) Yan, Y.; Qin, B.; Ren, C. L.; Chen, X. Y.; Yip, Y. K.; Ye, R. J.; Zhang, D. W.; Su, H. B.; Zeng, H. Q. *J. Am. Chem. Soc.* **2010**, *132*, 5869–5879; (c) Qin, B.; Ren, C. L.; Ye, R. J.; Sun, C.; Chiad, K.; Chen, X. Y.; Li, Z.; Xue, F.; Su, H. B.; Chass, G. A.; Zeng, H. Q. *J. Am. Chem. Soc.* **2010**, *132*, 9564–9566; (d) Qin, B.; Ong, W. Q.; Ye, R. J.; Du, Z. Y.; Chen, X. Y.; Yan, Y.; Zhang, K.; Su, H. B.; Zeng, H. Q. *Chem. Commun.* **2011**, 5419–5421; (e) Qin, B.; Sun, C.; Liu, Y.; Shen, J.; Ye, R. J.; Zhu, J.; Duan, X.-F.; Zeng, H. Q. *Org. Lett.* **2011**, *13*, 2270–2273.
24. Anelli, P. L.; Ashton, P. R.; Ballardini, R.; Balzani, V.; Delgado, M.; Gandolfi, M. T.; Goodnow, T. T.; Kaifer, A. E.; Philp, D.; Pietraszkiewicz, M.; Prodi, L.; Reddington, M. V.; Slawin, A. M. Z.; Spencer, N.; Stoddart, J. F.; Vicent, C.; Williams, D. J. *J. Am. Chem. Soc.* **1992**, *114*, 193–218.
25. Liu, Y.; Flood, A. H.; Bonvallet, P. A.; Vignon, S. A.; Northrop, B. H.; Tseng, H.-R.; Jeppesen, J. O.; Huang, T. J.; Brough, B.; Baller, M.; Magonov, S.; Solares, S. D.; Goddard, W. A.; Ho, C.-M.; Stoddart, J. F. *J. Am. Chem. Soc.* **2005**, *127*, 9745–9759.
26. Jia, C.; Zhang, D.; Xu, W.; Zhu, D. *Org. Lett.* **2001**, *3*, 1941–1944.
27. The samples of **1b**–**d** were found stable at room temperature after two months. The ^1H NMR spectra of their suspended solution in $CDCl_3$ did not exhibit the signals of free **3b**–**d**, and the thin layer chromatography (TLC) did not show the spot of free **3b**–**d** either.
28. The 1:1 mixture of **3a** and $CBPQT{\cdot}4PF_6$ in acetonitrile/acetone (1:2, v/v) quickly turned from orange to blue, indicating the formation of the threaded complex. However, the trituration of the concentrated residue with acetonitrile/water (1:4, v/v) or dichloromethane/petroleum ether (1:2, v/v) caused complete removal of $CBPQT{\cdot}4PF_6$ and **3a**, respectively, indicating that pseudorotaxane **1a** decomplexed rapidly within the operation time.
29. Tseng, H. R.; Vignon, S. A.; Stoddart, J. F. *Angew. Chem., Int. Ed.* **2003**, *42*, 1491–1495.
30. Ashton, P. R.; Baxter, I.; Fyfe, M. C. T.; Raymo, F. M.; Spencer, N.; Stoddart, J. F.; White, A. J. P.; Williams, D. J. *J. Am. Chem. Soc.* **1998**, *120*, 2297–2307.
31. Chiang, P.-T.; Cheng, P.-N.; Lin, C.-F.; Liu, Y.-H.; Lai, C.-C.; Peng, S.-M.; Chiu, S.-H. *Chem.—Eur. J.* **2006**, *12*, 865–876.
32. Reichardt, C. *Solvents and Solvent Effects in Organic Chemistry*; Wiley-VCH: Weinheim, 2003; 653.
33. (a) Parra, R. D.; Zeng, H.; Zhu, J.; Zheng, C.; Zeng, X. C.; Gong, B. *Chem.—Eur. J.* **2001**, *7*, 4352–4357; (b) Jiang, H.; Léger, J. M.; Guionneau, P.; Huc, I. *Org. Lett.* **2004**, *6*, 2985–2988; (c) Li, F.; Gan, Q.; Xue, L.; Wang, Z.-M.; Jiang, H. *Tetrahedron Lett.* **2009**, *50*, 2367–2369.
34. Connelly, N. G.; Geiger, W. *Chem. Rev.* **1996**, *96*, 877–910.
35. Kanamori, D.; Okamura, T.-A.; Yamamoto, H.; Ueyama, N. *Angew. Chem., Int. Ed.* **2005**, *44*, 969–972.
36. Yu, Z.; Hecht, S. *Angew. Chem., Int. Ed.* **2011**, *50*, 1640–1643.
37. Hou, J.-L.; Shao, X.-B.; Chen, G.-J.; Zhou, Y.-X.; Jiang, X.-K.; Li, Z.-T. *J. Am. Chem. Soc.* **2004**, *126*, 12386–12394.